Observation of Light Thermalization to Negative-Temperature Rayleigh-Jeans Equilibrium States in Multimode Optical Fibers

K. Baudin,[1,2] J. Garnier,[2] A. Fusaro,[3] N. Berti,[1] C. Michel,[4] K. Krupa,[5] G. Millot,[1,6] and A. Picozzi[1]
[1]*Laboratoire Interdisciplinaire Carnot de Bourgogne, CNRS, Université de Bourgogne, Dijon, France*
[2]*CMAP, CNRS, Ecole Polytechnique, Institut Polytechnique de Paris, 91128 Palaiseau Cedex, France*
[3]*CEA, DAM, DIF, F-91297 Arpajon Cedex, France*
[4]*Université Côte d'Azur, CNRS, Institut de Physique de Nice, Nice, France*
[5]*Institute of Physical Chemistry Polish Academy of Sciences, Warsaw, Poland*
[6]*Institut Universitaire de France (IUF), 1 rue Descartes, 75005 Paris, France*

(Received 22 July 2022; accepted 3 January 2023; published 8 February 2023)

Although the temperature of a thermodynamic system is usually believed to be a positive quantity, under particular conditions, negative-temperature equilibrium states are also possible. Negative-temperature equilibriums have been observed with spin systems, cold atoms in optical lattices, and two-dimensional quantum superfluids. Here we report the observation of Rayleigh-Jeans thermalization of light waves to negative-temperature equilibrium states. The optical wave relaxes to the equilibrium state through its propagation in a multimode optical fiber—i.e., in a conservative Hamiltonian system. The bounded energy spectrum of the optical fiber enables negative-temperature equilibriums with high energy levels (high-order fiber modes) more populated than low energy levels (low-order modes). Our experiments show that negative-temperature speckle beams are featured, in average, by a nonmonotonic radial intensity profile. The experimental results are in quantitative agreement with the Rayleigh-Jeans theory without free parameters. Bringing negative temperatures to the field of optics opens the door to the investigation of fundamental issues of negative-temperature states in a flexible experimental environment.

DOI: 10.1103/PhysRevLett.130.063801

Introduction.—Temperature is a central concept of statistical mechanics and often reflects a measure of the amount of disordered motion in a classical ideal gas. Although this intuitive notion is correct for many physical systems, one should keep in mind that the concept of temperature is by far more subtle. A detailed analysis of the concept of temperature, and of its relationship with energy and entropy shows that, under suitable conditions, the entropy can decrease with the energy, thus allowing for the existence of equilibrium states at negative temperatures (NTs). Starting from the seminal works by Onsager [1] and Ramsey [2], who originally conceived the physical idea and the first theoretical approaches, during the last few decades, many works have been devoted to the theoretical understanding of these unusual equilibrium states. Despite the fact that the existence of a NT equilibrium has created its own share of confusion in relation with the definition of the entropy [3,4], NTs are now broadly accepted in line with different experimental observations [5–12]. NTs were originally observed experimentally in nuclear spin systems [13]. More recently, NTs were observed with cold atoms in optical lattices [14]. Furthermore, NTs originally predicted by Onsager in the statistical description of point vortices [1] have been recently observed in 2D quantum superfluids [15,16].

In this Letter, we present an experimental optical setup in which we report the observation of light thermalization to NT equilibrium states. Our system is based on the nonlinear propagation of speckle beams in a multimode optical fiber (MMF). Because of the presence of a finite number of modes supported by the MMF, the spectrum exhibits both lower and upper bounds for the energy levels. The bounded spectrum, combined to the nonlinear four-wave interaction, are responsible for the process of Rayleigh-Jeans (RJ) thermalization to NT equilibrium states [17,18]. We stress that, at variance with other experiments where photon thermalization is driven by a thermal heat bath [19–22], here light thermalization takes place in a conservative Hamiltonian system. RJ thermalization to usual *positive-temperature* equilibriums has been recently demonstrated experimentally in MMFs [23–26], on the basis of a spatial beam-cleaning effect [27–31]. As described by the wave turbulence theory [32–36] applied to MMFs [37–40], the thermalization to a positive-temperature equilibrium is characterized by a transfer of power (particle number) toward the low-order modes of the MMF. In marked contrast, here we report the observation of thermalization to a NT equilibrium featured by a power transfer to high-order modes (direct flow of particles), as well as a transfer of energy to low-order modes (inverse flow of energy). Consequently, the NT equilibrium is characterized by an inverted modal population, in which high-order modes are more populated than low-order modes.

 © 2023 American Physical Society

Our experimental optical setup can be used as a simple and flexible testbed to explore fundamental issues related to NT states that are discussed in conclusion—e.g., Carnot cycles operating between temperatures of opposite signs, or inverted turbulence cascades featured by an analogue process of condensation at NT.

Experimental system.—The experiment is based on the single-pass propagation of speckle beams through a MMF. The subnanosecond pulses delivered by a Nd:YAG laser ($\lambda = 1.06$ μm) are transmitted through a spiral phase plate and then through a diffuser before injection of the speckle beam into a 12 m–long graded-index MMF (i.e., parabolic-shaped trapping potential), which guides $M = 45$ modes—i.e., nine groups of degenerate modes. The energy levels (fiber eigenvalues) are well approximated by those of a harmonic potential $\beta_p = \beta_0(p_x + p_y + 1)$, where $\{p\}$ labels the two integers (p_x, p_y) that specify a mode [41]. We denote by $|a_p|^2$ the power in the mode p, with the total power $N = \sum_p |a_p|^2$ [45].

The experiment is realized in the weakly nonlinear regime, where linear effects dominate over nonlinear effects: $L_{\rm lin} \sim \beta_0^{-1} \sim 0.1$ mm $\ll L_{\rm nl} = 1/(\gamma N) \sim 20$ cm, with γ being the nonlinear coefficient of the MMF. Accordingly, we do not consider NT states associated with nonlinear coherent structures—e.g., breathers [10,48,49]. Since $L_{\rm lin} \ll L_{\rm nl}$, we only retain the linear contribution to the Hamiltonian, $E = \sum_p \beta_p |a_p|^2$ [23–25]. We have verified the conservation of the power N and the energy E through propagation in the NT region for each realization of a speckle beam, which confirms that the coupling between guided modes and leaky modes of the fiber can be neglected [41].

RJ thermalization is driven by the four-wave nonlinear interaction through the propagation in the MMF. The speckle beam is expected to relax toward the thermodynamic equilibrium state described by the RJ distribution [17,23–25,38,39]:

$$n_p^{\rm RJ} = T/(\beta_p - \mu), \tag{1}$$

where T and μ are the temperature and chemical potential, while $n_p = \langle |a_p|^2 \rangle$ denotes the modal power averaged over the realizations of the speckle beams. We have at equilibrium $N = T\sum_p (\beta_p - \mu)^{-1}$ and $E = T\sum_p \beta_p/(\beta_p - \mu)$, with (T, μ) uniquely determined by (N, E)—we deal with a microcanonic description (T is not defined by a thermostat; it is in units of $\mathrm{W}\cdot\mathrm{m}^{-1}$) [36]. Note that the RJ distribution refers to the classical, low-energy limit of the Bose-Einstein distribution [32], describing highly occupied fiber modes.

Negative temperatures.—The irreversible process of RJ thermalization is described by the wave turbulence theory [32–36], which provides a nonequilibrium description of light propagation in MMFs [37–40]. An equilibrium thermodynamic formulation of multimode optical systems has been recently developed [17,50]. We report in Fig. 1 the relative entropy $S = \sum_p \log(n_p^{\rm RJ})$ as a function of the energy for the MMF used in our experiments with $g = 9$ groups of degenerate modes. Because the spectrum of the fiber is bounded, $\beta_0 \le \beta_p \le \beta_{\rm max} = g\beta_0$, the system possesses both lower and upper energy bounds:

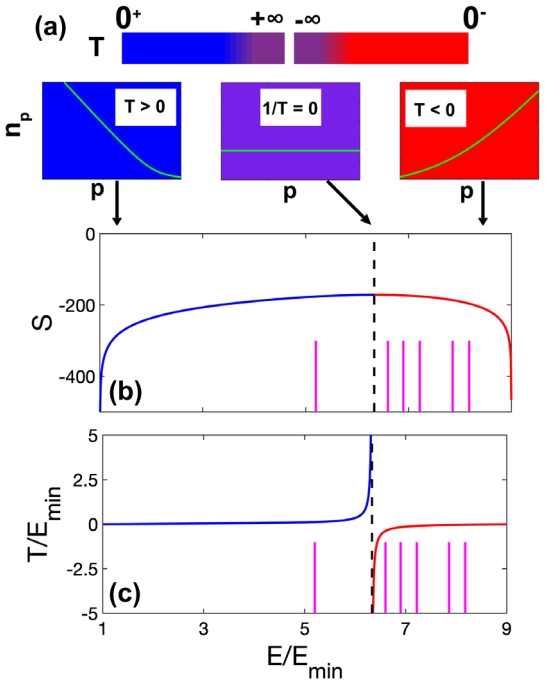

FIG. 1. Negative temperatures and inverted modal population. (a) RJ equilibrium distribution $n_p^{\rm RJ}$ for positive temperature $T > 0$ ($E < E_*$), where low-order modes are more populated, and negative temperatures $T < 0$ ($E > E_*$), featured by an inverted modal population, while for $1/T \to 0$ ($E = E_*$), $n_p^{\rm RJ} = \text{const}$. (b) Relative entropy S vs energy E, showing that $1/T = (\partial S/\partial E)_{N,M} < 0$ requires $E > E_*$. (c) Temperature T vs energy E. Negative temperatures $T < 0$ occur for $E > E_*$ with $E_*/E_{\rm min} \simeq 6.33$ (vertical dashed black line). The vertical purple lines in (b) and (c) denote the six values of E considered in Fig. 2.

$$E_{\rm min} = N\beta_0 \le E \le E_{\rm max} = N\beta_{\rm max}. \tag{2}$$

Starting at minimum energy $E_{\rm min}$, where only the fundamental mode is populated, an increase in energy leads to an occupation of a larger number of fiber modes and therefore an increase in entropy. As the temperature approaches infinity, all fiber modes become equally populated, $n_p^{\rm RJ} = \text{const}$, and the entropy reaches a maximum for $E = E_* = N\langle\beta_p\rangle = E_{\rm min}(2g+1)/3$. NT equilibrium states arise for $E > E_*$, where the entropy decreases by increasing the energy, $1/T = (\partial S/\partial E)_{M,N} < 0$. The condition $E > E_*$ can be achieved if high-order modes are more populated than low-order modes. Note that NT equilibrium states persist in the thermodynamic limit [41].

RJ thermalization to NT equilibriums.—At variance with usual experiments of spatial beam cleaning and RJ

thermalization [24–30], here we study the thermalization for different values of the energy E, while keeping constant the power N. Indeed, by passing the laser beam through a diffuser before injection into the fiber, we can vary the amount of randomness of the speckle beam by keeping $N = \text{const}$: the larger the randomness of the speckle beam, the higher the energy E. Accordingly, we study RJ thermalization over a broad range of variation of the energy. In order to further increase the energy beyond the threshold for NT ($E > E_*$), we pass the beam through a spiral phase plate before the diffuser—i.e., we generate a speckle beam from a doughnut-like intensity distribution, which enables the excitation of higher-order fiber modes.

The accurate measurements of the near-field and far-field intensity distributions allowed us to retrieve the modal power distribution n_p^{exp}. To obtain the mode decomposition, several interferometric approaches based on the use of a reference beam have been exploited to study light thermalization in MMFs [24–26]. Here, in contrast to previous works [23–26], we use a noninterferometric numerical mode decomposition procedure that is based on the Gerchberg-Saxton algorithm. It allows us to retrieve the transverse phase profile of the speckle field from the near-field and far-field intensity distributions measured in the experiments [46,47,51,52]. By projecting the retrieved complex field over the fiber modes, we get the complete modal distribution.

The RJ distribution being in essence a statistical distribution, its comparison with the experiments requires an average over realizations of speckle beams. We have recorded 2×300 realizations of the near-field and far-field intensity distributions for the same power ($N = 7$ kW) and different energies E. For each individual speckle realization, we retrieve the modal distribution $|a_p^{\text{exp}}|^2$. We partition the ensemble of 300 realizations of $\{|a_p^{\text{exp}}|^2\}$ within small energy intervals $[E - \Delta E, E + \Delta E]$ with $\Delta E = 0.125 E_{\text{min}}$. We perform an average over the realizations of the modal distributions for each energy interval, which provides the averaged modal distribution $n_p^{\text{exp}} = \langle |a_p^{\text{exp}}|^2 \rangle$. This procedure is applied at the fiber output ($L = 12$ m) and the fiber input (after 20 cm of propagation). The error in the procedure has been computed theoretically and numerically; it decreases with the number of realizations and has been found to be remarkably small (relative standard deviations of $\simeq 6\%$) [41].

We report in Fig. 2 the averaged modal distributions n_p^{exp} at the fiber input (blue) and output (red), for different values of the energy E, or equivalently the temperature T [purple lines in Figs. 1(b) and 1(c)]. The data are compared with the theoretical RJ distribution n_p^{RJ}. We stress that there are no adjustable parameters between n_p^{exp} and n_p^{RJ}: The parameters (T, μ) in n_p^{RJ} are uniquely determined by N and E measured in the experiments. We observe in Fig. 2 an excellent agreement between n_p^{exp} (red circles) and n_p^{RJ} (green line), for both $T > 0$ and $T < 0$. Figure 2 then shows

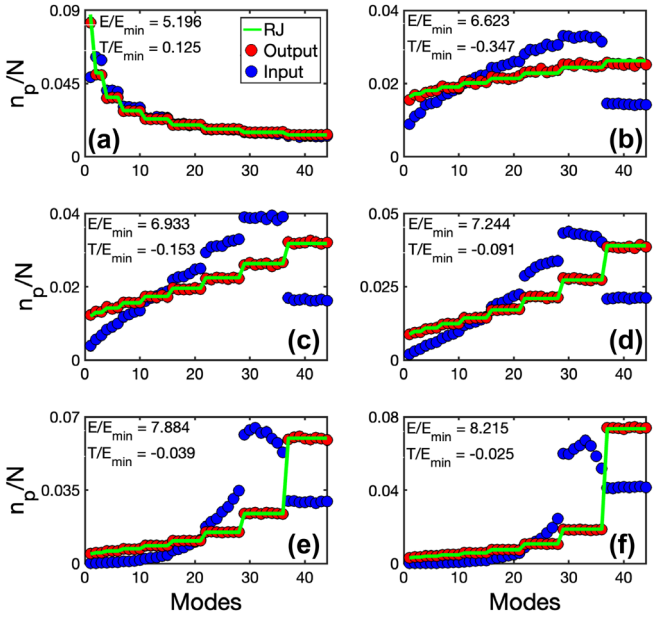

FIG. 2. Rayleigh-Jeans thermalization to NT equilibriums. Experimental modal distributions averaged over realizations $n_p^{\text{exp}} = \langle |a_p^{\text{exp}}|^2 \rangle$ at the fiber input (blue), and at the fiber output (red). Also shown is the corresponding RJ equilibrium distribution n_p^{RJ} (green). Note the quantitative agreement between n_p^{RJ} and the experimental output distribution n_p^{exp} (red). The six panels correspond to different values of E, or equivalently different T; see the six vertical purple lines in Figs. 1(b) and 1(c). The modal distribution peaked on the lowest mode for (a) $T > 0$ gets inverted for (b)–(f) $T < 0$. An average over $\simeq 35$ realizations of speckle beams is considered for each panel. The fiber modes are sorted from the fundamental one (β_0) to the highest-mode group (ninefold degenerate with $\beta_{\text{max}} = 9\beta_0$). Degenerate modes are equally populated at equilibrium, leading to a staircase distribution n_p^{RJ}.

that NT equilibriums constitute *attractor states* for the random wave, whose robustness has a thermodynamic origin—the maximum entropy state for a given pair (N, E).

Energy flows in mode space.—The conventional thermalization to positive temperatures is characterized by an energy flow to high-order modes [33,34,38]. Thermalization to NTs typically occurs through an inverse energy flow to low-order modes [18]. This is illustrated in Fig. 3, which shows that the energy distribution $\varepsilon_p^{\text{exp}} = \beta_p n_p^{\text{exp}}$ at low-order modes increases through propagation in the MMF and reaches the theoretical RJ equilibrium distribution $\varepsilon_p^{\text{RJ}} = \beta_p n_p^{\text{RJ}}$.

Oscillating radial intensity distribution.—The intensity distribution $I^{\text{RJ}}(\boldsymbol{r})$ of usual positive-temperature equilibriums is, in average, a monotonic decreasing function with the radial distance $|\boldsymbol{r}|$ [23]. This is consistent with the intuitive idea that low-order modes localized near the fiber center are the most populated ones. In marked contrast, the inverted modal population of NT equilibriums is characterized by an oscillating behavior of the radial intensity

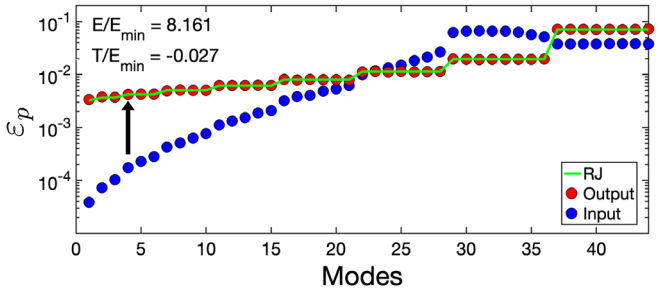

FIG. 3. Energy flows in mode space. Experimental energy distributions averaged over 50 realizations $\varepsilon_p^{\rm exp} = \beta_p n_p^{\rm exp}$, at the fiber input (blue) and output (red). The arrow indicates the energy flow to low-order modes. Also shown is the corresponding RJ equilibrium distribution $\varepsilon_p^{\rm RJ} = \beta_p n_p^{\rm RJ}$ (green line), which is in quantitative agreement with the experimental output distribution (red).

distribution. This is illustrated in Fig. 4, which reports the averaged radial intensity distribution $I^{\rm exp}(\boldsymbol{r})$ (with $\Delta E = 0.25 E_{\rm min}$, $E/E_{\rm min} = 7.9$). The theoretical RJ intensity distribution reads

$$I^{\rm RJ}(\boldsymbol{r}) = \sum_p n_p^{\rm RJ} u_p^2(\boldsymbol{r}), \tag{3}$$

where $u_p(\boldsymbol{r})$ denotes the fiber modes [23]. The number of radial oscillations in Fig. 4 is given by the most oscillating mode of the fiber—namely, the mode LP_{04} that exhibits five oscillations.

Experiments by increasing power.—We have studied the optical field at the output of the MMF, with a small power $N = 0.23$ kW (linear regime), and a high power $N = 7$ kW (nonlinear regime). Since the MMF length is kept fixed ($L = 12$ m), the effective number of nonlinear interaction lengths increases by increasing the power. Figure 5 reports the fraction of power that populates the highest group of degenerate modes of the MMF, $\tilde{n}_g/N$ for $g = 9$. The output field (red) reaches the equilibrium RJ theory (green line) in the nonlinear regime. The highest energy level gets macroscopically populated by increasing the energy, or equivalently by increasing the negative temperature (see Fig. 1).

Conclusion and perspectives.—We have reported the observation of RJ thermalization to NT equilibrium states through light propagation in graded-index MMFs. This nonequilibrium process of NT thermalization can be described by a wave turbulence kinetic equation, which is found to be in agreement with the simulations of the nonlinear Schrödinger equation [41]. Our NT experiment then paves the way for the study of Zakharov-Kolmogorov turbulence cascades [32–34] that are inverted with respect to those underlying usual positive-temperature thermalization (e.g., inverse energy flow in Fig. 3).

Along this line, our Letter suggests a previously unrecognized process of inverted condensation at NTs: At variance with usual condensation at positive temperature where the lowest energy level gets macroscopically populated by *decreasing* the temperature ($T \to 0^+$, or $E \to E_{\rm min}$) [23,33–36], at NT an inverted condensation process occurs into the highest energy level as the temperature *increases to zero* ($T \to 0^-$, or $E \to E_{\rm max}$). While we provide a preliminary study of this effect through the macroscopic population of the highest energy level (Fig. 5), the observation of the transition to condensation requires MMFs with a larger number of modes [41].

In our Letter, NT states are obtained directly, which is in contrast with magnetic systems and cold atoms, where the excitation of NT states requires first the creation of a positive-temperature state and then its subsequent inversion through suitable procedures (magnetic field inversion or Feshbach resonances). This opens the possibility to study the physics of NT in a flexible experimental environment. For instance, the thermalization of two beams at different

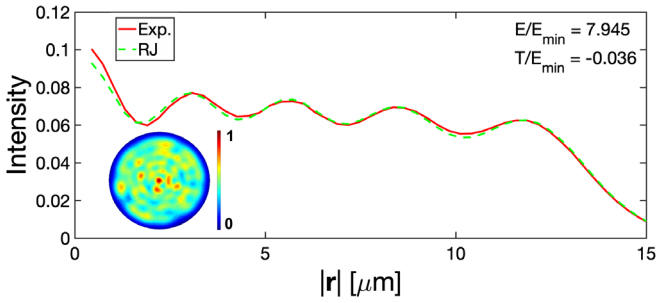

FIG. 4. Oscillating radial intensity distribution at NT. Intensity distribution $I^{\rm exp}(\boldsymbol{r})$ averaged over the realizations and over angle as a function of the radial distance $|\boldsymbol{r}|$ (red). Note the quantitative agreement with the theoretical RJ intensity distribution $I^{\rm RJ}(\boldsymbol{r})$ in Eq. (3) (dashed green). The oscillating behavior of the intensity distribution is a signature of the NT equilibrium. *Inset:* corresponding 2D intensity averaged over the realizations (the radius of the circle is the fiber radius).

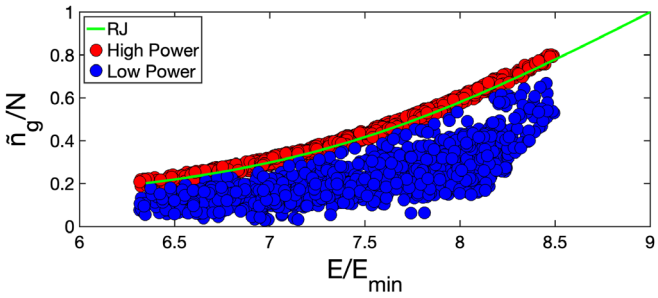

FIG. 5. Macroscopic population of the highest energy level. Fraction of power $\tilde{n}_g/N$ into the highest mode group $g = 9$ vs energy $E/E_{\rm min}$. Experimental measurements at the fiber output: The blue circles refer to the linear regime (small power), and the red circles to the nonlinear regime (high power). The green line denotes the RJ equilibrium theory. By increasing the energy, the power goes to the highest energy level, $\tilde{n}_g/N \to 1$ as $E/E_{\rm min} \to 9$.

laser wavelengths interacting through the fiber nonlinearity can be exploited to achieve an efficient optical refrigeration: A highly incoherent speckled beam at NT can be cooled through its thermalization with a coherent beam towards a highly coherent state without any power loss. In contrast with usual beam cleaning at positive temperature where the energy is conserved, here the cooling process is featured by an energy transfer from the incoherent to the coherent beam, which significantly improves the gain of coherence of the incoherent beam. Following this idea, one can explore the meaning of a *thermostat at NT* [10]: If the NT incoherent beam has a power much larger than the partially coherent beam, it will play the role of a NT thermal reservoir for such a partially coherent beam.

The versatile optical experimental environment proposed in this Letter also opens the possibility to study controversies about NTs, such as thermodynamic engines featured by Carnot cycles operating between temperatures of opposite signs, in relation with the generalized Kelvin-Planck formulation of the second law of thermodynamics stating that it is not possible to completely transform work into heat at NT [10].

The authors are grateful to S. Rica, I. Carusotto, and V. Doya for fruitful discussions. Funding was provided by the Centre national de la recherche scientifique (CNRS), Conseil régional de Bourgogne Franche-Comté, iXCore Research Fondation, and Agence Nationale de la Recherche (Grants No. ANR-19-CE46-0007, No. ANR-15-IDEX-0003, and No. ANR-21-ESRE-0040). Calculations were performed using HPC resources from DNUM CCUB (Centre de Calcul, Université de Bourgogne).

[1] L. Onsager, Statistical hydrodynamics, Il Nuovo Cimento (1943–1954) **6**, 279 (1949).
[2] N. F. Ramsey, Thermodynamics and statistical mechanics at negative absolute temperatures, Phys. Rev. **103**, 20 (1956).
[3] J. Dunkel and S. Hilbert, Consistent thermostatistics forbids negative absolute temperatures, Nat. Phys. **10**, 67 (2014).
[4] S. Calabrese and A. Porporato, Origin of negative temperatures in systems interacting with external fields, Phys. Lett. A **383**, 2153 (2019).
[5] D. Frenkel and P. B. Warren, Gibbs, Boltzmann, and negative temperatures, Am. J. Phys. **83**, 163 (2015).
[6] P. Buonsante, R. Franzosi, and A. Smerzi, On the dispute between Boltzmann and Gibbs entropy, Ann. Phys. (Amsterdam) **375**, 414 (2016).
[7] A. Puglisi, A. Sarracino, and A. Vulpiani, Temperature in and out of equilibrium: A review of concepts, tools and attempts, Phys. Rep. **709**, 1 (2017).
[8] L. Cerino, A. Puglisi, and A. Vulpiani, A consistent description of fluctuations requires negative temperatures, J. Stat. Mech. (2015) P12002.
[9] E. Abraham and O. Penrose, Physics of negative absolute temperatures, Phys. Rev. E **95**, 012125 (2017).
[10] M. Baldovin, S. Iubini, R. Livi, and A. Vulpiani, Statistical mechanics of systems with negative temperature, Phys. Rep. **923**, 1 (2021).
[11] M. Onorato, G. Dematteis, D. Proment, A. Pezzi, M. Ballarin, and L. Rondoni, Equilibrium and nonequilibrium description of negative temperature states in a one-dimensional lattice using a wave kinetic approach, Phys. Rev. E **105**, 014206 (2022).
[12] Note that particles in a laser have an inverted energy population, which, however, only exists as long as the laser is continuously pumped (by switching off the pump, all atoms decay back into the lower state, and their energy goes into the laser beam). The laser medium is in a steady state, but not in thermal equilibrium, and therefore it cannot have a temperature.
[13] E. M. Purcell and R. V. Pound, A nuclear spin system at negative temperature, Phys. Rev. **81**, 279 (1951).
[14] S. Braun, J. P. Ronzheimer, M. Schreiber, S. S. Hodgman, T. Rom, I. Bloch, and U. Schneider, Negative absolute temperature for motional degrees of freedom, Science **339**, 52 (2013).
[15] S. P. Johnstone, A. J. Groszek, P. T. Starkey, C. J. Billington, T. P. Simula, and K. Helmerson, Evolution of large-scale flow from turbulence in a two-dimensional superfluid, Science **364**, 1267 (2019).
[16] G. Gauthier, M. T. Reeves, X. Yu, A. S. Bradley, M. A. Baker, T. A. Bell, H. Rubinsztein-Dunlop, M. J. Davis, and T. W. Neely, Giant vortex clusters in a two-dimensional quantum fluid, Science **364**, 1264 (2019).
[17] F. O. Wu, A. U. Hassan, and D. N. Christodoulides, Thermodynamic theory of highly multimoded nonlinear optical systems, Nat. Photonics **13**, 776 (2019).
[18] K. Baudin, A. Fusaro, J. Garnier, N. Berti, K. Krupa, I. Carusotto, S. Rica, G. Millot, and A. Picozzi, Energy and wave-action flows underlying Rayleigh-Jeans thermalization of optical waves propagating in a multimode fiber, Europhys. Lett. **134**, 14001 (2021).
[19] C. Conti, M. Leonetti, A. Fratalocchi, L. Angelani, and G. Ruocco, Condensation in Disordered Lasers: Theory, 3D + 1 Simulations, and Experiments, Phys. Rev. Lett. **101**, 143901 (2008).
[20] J. Klaers, J. Schmitt, F. Vewinger, and M. Weitz, Bose-Einstein condensation of photons in an optical microcavity, Nature (London) **468**, 545 (2010).
[21] R. Weill, A. Bekker, B. Levit, and B. Fischer, Bose-Einstein condensation of photons in an erbium-ytterbium co-doped fiber cavity, Nat. Commun. **10**, 747 (2019).
[22] J. Bloch, I. Carusotto, and M. Wouters, Nonequilibrium Bose-Einstein condensation in photonic systems, Nat. Phys. Rev. **4**, 470 (2022).
[23] K. Baudin, A. Fusaro, K. Krupa, J. Garnier, S. Rica, and G. Millot, A. Picozzi, Classical Rayleigh-Jeans Condensation of Light Waves: Observation and Thermodynamic Characterization, Phys. Rev. Lett. **125**, 244101 (2020).
[24] H. Pourbeyram, P. Sidorenko, F. Wu, L. Wright, D. Christodoulides, and F. Wise, Direct observations of thermalization to a Rayleigh–Jeans distribution in multimode optical fibres, Nat. Phys. **18**, 685 (2022).
[25] F. Mangini, M. Gervaziev, M. Ferraro, D. S. Kharenko, M. Zitelli, Y. Sun, V. Couderc, E. V. Podivilov, S. A. Babin, and S. Wabnitz, Statistical mechanics of beam self-cleaning in

GRIN multimode optical fibers, Opt. Express **30**, 10850 (2022).
[26] E. V. Podivilov, F. Mangini, O. S. Sidelnikov, M. Ferraro, M. Gervaziev, D. S. Kharenko, M. Zitelli, M. P. Fedoruk, S. A. Babin, and S. Wabnitz, Thermalization of Orbital Angular Momentum Beams in Multimode Optical Fibers, Phys. Rev. Lett. **128**, 243901 (2022).
[27] Z. Liu, L. G. Wright, D. N. Christodoulides, and F. W. Wise, Kerr self-cleaning of femtosecond-pulsed beams in graded-index multimode fiber, Opt. Lett. **41**, 3675 (2016).
[28] L. G. Wright, Z. Liu, D. A. Nolan, M.-J. Li, D. N. Christodoulides, and F. W. Wise, Self-organized instability in graded-index multimode fibres, Nat. Photonics **10**, 771 (2016).
[29] K. Krupa, A. Tonello, B. M. Shalaby, M. Fabert, A. Barthélémy, G. Millot, S. Wabnitz, and V. Couderc, Spatial beam self-cleaning in multimode fibres, Nat. Photonics **11**, 237 (2017).
[30] E. Podivilov, D. Kharenko, V. Gonta, K. Krupa, O. S. Sidelnikov, S. Turitsyn, M. P. Fedoruk, S. A. Babin, and S. Wabnitz, Hydrodynamic 2D Turbulence and Spatial Beam Condensation in Multimode Optical Fibers, Phys. Rev. Lett. **122**, 103902 (2019).
[31] A. Ramos, L. Fernández-Alcázar, T. Kottos, and B. Shapiro, Optical Phase Transitions in Photonic Networks: A Spin-System Formulation, Phys. Rev. X **10**, 031024 (2020).
[32] V. E. Zakharov, V. S. L'vov, and G. Falkovich, *Kolmogorov Spectra of Turbulence I* (Springer, Berlin, 1992).
[33] S. Nazarenko, *Wave Turbulence*, Lectures Notes in Physics (Springer, New York, 2011).
[34] A. C. Newell and B. Rumpf, Wave turbulence, Annu. Rev. Fluid Mech. **43**, 59 (2011).
[35] J. Laurie, U. Bortolozzo, S. Nazarenko, and S. Residori, One-dimensional optical wave turbulence: Experiment and theory, Phys. Rep. **514**, 121 (2012).
[36] A. Picozzi, J. Garnier, T. Hansson, P. Suret, S. Randoux, G. Millot, and D. N. Christodoulides, Optical wave turbulence: Toward a unified nonequilibrium thermodynamic formulation of statistical nonlinear optics, Phys. Rep. **542**, 1 (2014).
[37] P. Aschieri, J. Garnier, C. Michel, V. Doya, and A. Picozzi, Condensation and thermalization of classical optical waves in a waveguide, Phys. Rev. A **83**, 033838 (2011).
[38] A. Fusaro, J. Garnier, K. Krupa, G. Millot, and A. Picozzi, Dramatic Acceleration of Wave Condensation Mediated by Disorder in Multimode Fibers, Phys. Rev. Lett. **122**, 123902 (2019).
[39] J. Garnier, A. Fusaro, K. Baudin, C. Michel, K. Krupa, G. Millot, and A. Picozzi, Wave condensation with weak disorder versus beam self-cleaning in multimode fibers, Phys. Rev. A **100**, 053835 (2019).
[40] N. Berti, K. Baudin, A. Fusaro, G. Millot, A. Picozzi, and J. Garnier, Interplay of thermalization and strong disorder: Wave Turbulence Theory, Numerical Simulations, and Experiments in Multimode Optical Fibers, Phys. Rev. Lett. **129**, 063901 (2022).
[41] See Supplemental Material at http://link.aps.org/supplemental/10.1103/PhysRevLett.130.063801 for the experimental procedures (including the measurement of E, the conservation of E and N through propagation in the MMF, the estimation of the error in the modal decomposition), for the thermodynamic relations plotted in Fig. 1, and the numerical simulations of the nonlinear Schrödinger equation and the wave turbulence kinetic equation, which includes Refs. [23,38,39,42–47].
[42] J. R. Fienup, Reconstruction of an object from the modulus of its Fourier transform, Opt. Lett. **3**, 27 (1978).
[43] S. Mumtaz, R. J. Essiambre, and G. P. Agrawal, Nonlinear propagation in multimode and multicore fibers: Generalization of the Manakov equations, J. Lightwave Technol. **31**, 398 (2013).
[44] A. Biasi, O. Evnin, and B. A. Malomed, Fermi-Pasta-Ulam phenomena and persistent breathers in the harmonic trap, Phys. Rev. E **104**, 034210 (2021).
[45] G. P. Agrawal, *Nonlinear Fiber Optics*, 6th ed. (Academic Press, New York, 2019).
[46] J. R. Fienup, Phase retrieval algorithms: A comparison, Appl. Opt. **21**, 2758 (1982).
[47] Y. Shechtman, Y. C. Eldar, O. Cohen, H. N. Chapman, J. Miao, and M. Segev, Phase retrieval with application to optical imaging: A contemporary overview, IEEE Signal Process. Mag. **32**, 87 (2015).
[48] B. Rumpf, Stable and metastable states and the formation and destruction of breathers in the discrete nonlinear Schrödinger equation, Physica (Amsterdam) **238D**, 2067 (2009).
[49] S. Iubini, L. Chirondojan, G.-L. Oppo, A. Politi, and P. Politi, Dynamical Freezing of Relaxation to Equilibrium, Phys. Rev. Lett. **122**, 084102 (2019).
[50] N. K. Efremidis and D. N. Christodoulides, Fundamental entropic processes in the theory of optical thermodynamics, Phys. Rev. A **103**, 043517 (2021).
[51] E. S. Manuylovich, V. V. Dvoyrin, and S. K. Turitsyn, Fast mode decomposition in few-mode fibers, Nat. Commun. **11**, 5507 (2020).
[52] O. Shapira, A. F. Abouraddy, J. D. Joannopoulos, and Y. Fink, Complete Modal Decomposition for Optical Waveguides, Phys. Rev. Lett. **94**, 143902 (2005).